Deep–Sea Research I 179 (2022) 103645

Contents lists available at ScienceDirect

Deep-Sea Research Part I

journal homepage: www.elsevier.com/locate/dsri

Linkages between sediment thickness, geomorphology and Mn nodule occurrence: New evidence from AUV geophysical mapping in the Clarion-Clipperton Zone

Evangelos Alevizos [a,*,1], Veerle A.I. Huvenne [a], Timm Schoening [b], Erik Simon-Lledó [a], Katleen Robert [a,c], Daniel O.B. Jones [a]

[a] National Oceanography Centre, Southampton, UK
[b] GEOMAR Helmholtz Centre for Ocean Research, Kiel, Germany
[c] School of Ocean Technology, Fisheries and Marine Institute of Memorial University, St. John's, NL, Canada

ARTICLE INFO

Keywords:
Deep sea
Mn nodules
Sub-bottom profiler
AUV imagery
Clarion-clipperton zone

ABSTRACT

The relationship between polymetallic nodules (Mn nodules) and deep-sea stratigraphy is relatively poorly studied and the role of sediment thickness in determining nodule occurrence is an active field of research. This study utilizes geophysical observations from three types of autonomous underwater vehicle (AUV) data (multi-beam bathymetry, sub-bottom profiles and underwater photography) in order to assess this relationship. Multi-beam bathymetry was processed with a pattern recognition approach for producing objective geomorphometric classes of the seafloor for examining their relation to sediment thickness and nodule occurrence. Sub-bottom profiles were used for extracting sediment thickness along a dense network of tracklines. Close-range AUV-photography data was used for automated counting of polymetallic nodules and their geometric features and it served as ground truth data. It was observed that higher nodule occurrence were related to layers with increased sediment thickness. This evidence reveals the role of local seafloor heterogeneity in nodule formation and suggests that unique patterns of local stratigraphy may affect geochemical processes that promote polymetallic nodule development at local scales.

1. Introduction

Seafloor exploration of deep-sea polymetallic nodule (Mn-nodules) fields has seen a significant, albeit sometimes discontinuous, development over the last decades. Earlier deep-sea surveys have led to acquisition of a large amount of baseline data for studying Mn-nodules and their relation to environmental parameters (e.g. sediment type, geochemistry) (ISA, 2010; Mewes et al., 2014) and benthic fauna (Simon-Lledó et al., 2019; Simon-Lledó et al., 2020; Amon et al., 2016). In recent years, modern autonomous underwater vehicle (AUV) technology has been applied in deep-sea mapping along with data acquisition techniques that provide a multitude of datasets simultaneously (Kwasnitschka et al., 2016; Morris et al., 2014; Wynn et al., 2014). High-resolution AUV-based data from multi-beam echo-sounders (MBES) and side-scan sonars (SSS) have been incorporated in recent mapping of Mn-nodule fields in the studies of Okazaki and Tsune (2013), Peukert et al. (2018) and Gazis et al. (2018) for example. These studies combined AUV-based bathymetry and SSS imagery with nodule metrics derived from automated analysis of AUV photographs (Schoening et al., 2016). Conventionally, geological and acoustic mapping of Mn-nodule fields have largely been based on morphological analysis of deep seafloor bathymetry, geo-acoustic data and/or underwater photography and physical sampling (de Moustier, 1985; Weydert, 1990; Chakraborty et al., 1996; Lee and Kim, 2004) at various scales, determined by the acquisition platform (i.e. ship-borne, AUV).

One of the least studied parameters in conjunction to Mn-nodule occurrence, however, is fine-scale stratigraphy. Most information about Mn-nodules and stratigraphy comes from studies of previous decades, based on shipboard sub-bottom profiler (SBP) and seismic records (Piper and Blueford, 1982; Usui and Tanahashi, 1986; Martin-Barajas

* Corresponding author.
E-mail address: evangelos.alevizos@noc.ac.uk (E. Alevizos).
[1] Current address: Institute of Mediterranean Studies (Foundation for Research and Technology Hellas), Nikiforou Foka 130, 74 100 Rethymno, PO BOX 119, Rethymno, Crete, Greece.ealevizos@ims.forth.gr

https://doi.org/10.1016/j.dsr.2021.103645
Received 4 February 2021; Received in revised form 14 October 2021; Accepted 18 October 2021
Available online 22 October 2021
0967-0637/

et al., 1991). There have been studies where increased nodule abundances were found on sloping seafloor and/or outcropping layers with thin sediment deposits (Glasby et al., 1982; Usui and Tanahashi 1986; Usui et al., 1993). However, there have been cases where higher nodule abundances were related with thick sediment accumulations (Moore and Heath 1966; Piper and Blueford 1982; Martin-Barajas et al., 1991). Furthermore, in the ISA report (2010) it is stated that the thickness of unconsolidated sediments in the CCZ (Korean contract area) corresponds with a negative trend in nodule metal content.

Local sedimentation rate is a less doubtful factor linked to nodule growth. In general, nodule development is favored by low sedimentation rates while high sedimentation rates tend to result in nodule-free areas (through nodule burial and subsequent dissolution) or small-sized nodules (Mewes et al., 2014). Sedimentation rates are generally low in the CCZ, and recent studies have shown that current sedimentation rates at the CCZ are 0.35 mm/year while a 2.5 million years ago hiatus in sedimentation has been identified (Mewes et al., 2014). Horst and graben lineaments characterize the CCZ seafloor surface and cause significant variability in local sedimentation rates by inducing altered bottom current speeds and directions (Mewes et al., 2014). In addition, being far from land (Smith and Demopoulos, 2003) and having low productivity surface waters (Pennington et al., 2006) also contribute in the relatively low sedimentation rates at the CCZ. Additionally, since the lower Miocene, the build-up of the eastern Antarctic ice cap intensified formation of Antarctic Bottom Water and led to the penetration of stronger currents into the equatorial North Pacific keeping the sedimentation rates low in the CCZ (Frazer and Fisk 1981; Piper and Blueford 1982; Glasby et al., 1982). Apart from sedimentation rates, sediment geochemistry is another important parameter that plays a vital role in nodule formation. However, there is a relatively small amount of literature about the geochemistry of the CCZ seafloor sediments. Mewes et al. (2014), suggest that when the Oxygen Penetration Depth (OPD) zone is limited then mobile Mn ions from the sedimentary column reach the seafloor surface and promote suboxic diagenetic nodule growth. They have also found that areas covered with small nodules or no nodules, contain an increased amount of fine-grained sediments (<6.3 μm) which are rich in refractory Mn phase. Thus, sediment graing size and lithology along with porous geochemistry are key factors in the development of Mn nodules.

Current datasets used in this study were collected in the frame of the MIDAS project which has been active from 2013 until 2016. The MIDAS project was an interdisciplinary work combining experts from all oceanographic aspects towards assessing the environmental impacts of activities linked to deep-sea mining (https://www.eu-midas.net/, accessed on July 01, 2021).

This study aims to assess the role of sediment thickness in nodule occurrence and to suggest potential strategies for future investigations. These tasks were facilitated by analysing high-resolution AUV multibeam echosounder and sub-bottom profiler data and AUV-based photography collected during the JC120 expedition in 2015 in the Clarion-Clipperton Zone (Fig. 1).

2. Materials and methods

2.1. Bathymetry data

During the JC120 cruise in 2015, on board the RRS *James Cook* (Jones et al., 2015), the AUV Autosub6000 was deployed for seven missions operating an EM2040 MBES sonar for high-resolution bathymetric mapping. The EM2040 was set at 200 kHz with survey altitudes at 50 m and 100 m above the seafloor surface. The MBES data were processed with the Caraibes software from IFREMER (Le Gal and Edy, 1997) to a grid with pixel size of 5 m × 5 m, and at the final stage ship-based bathymetry was used for spatial adjustment of the AUV bathymetry using ArcGIS. This was necessary since the AUV bathymetry was slightly misaligned owing to AUV inertial navigation issues. Clearly identifiable geomorphological points (e.g. top of steep hills or bottom of depressions) were used to georeference the AUV bathymetry to the shipboard data (see Jones et al., 2015). The AUV bathymetry map of the study area is shown in Fig. 2 and it is characterized mainly by elongated ridge features of N–S direction bounding a central valley formation mainly to the SE of the area. This site, an abyssal hill, has been termed the "ridge" area in other studies (e.g. Simon-Lledó et al., 2019; Jones et al., 2021). The study area is part of an Area of Particular Environmental Interest (APEI) designated by the International Seabed Authority (it is APEI-6). The APEI network includes a total of nine 400 × 400 km conservation areas that are protected from mining activity and they are geographically attached to the licensed areas (Shirayama et al., 2017; Jones et al.,2021).

This particular area shown in Fig. 1b was extensively covered by AUV-photography and dense SBP data during JC120. Thus, it was chosen as a baseline site for studying the potential relations between sub-bottom layers and Mn nodule occurrence. Although other APEI-6 areas have been also surveyed with AUV-photography there are no adequate, corresponding SBP data for supporting this study.

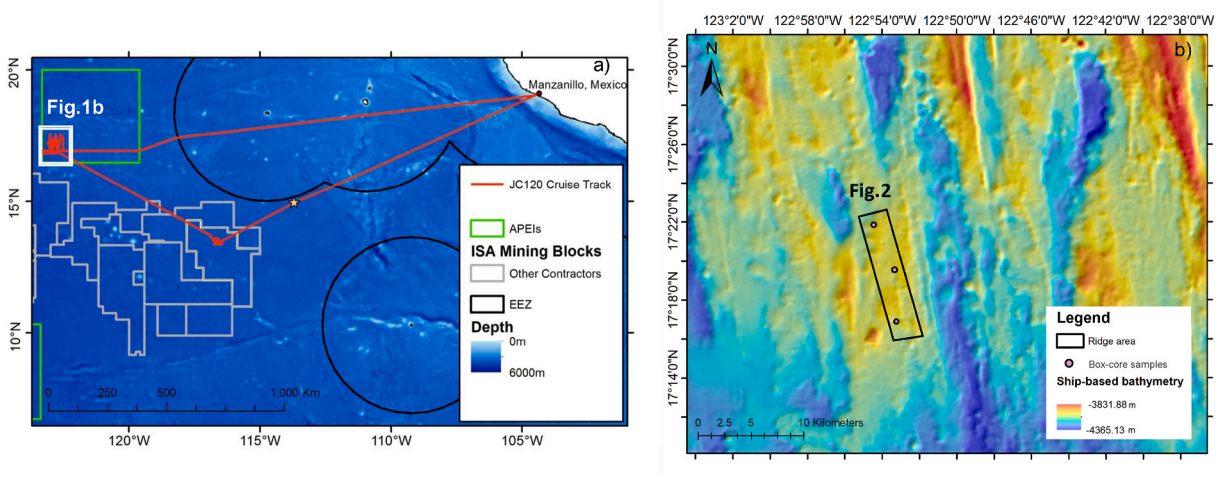

Fig. 1. a) The CCZ area with polygons highlighting the mining contract areas (from Jones et al., 2015), b) Ship-based multi-beam bathymetry of the wider study area shown with the black rectangle representing the study area.

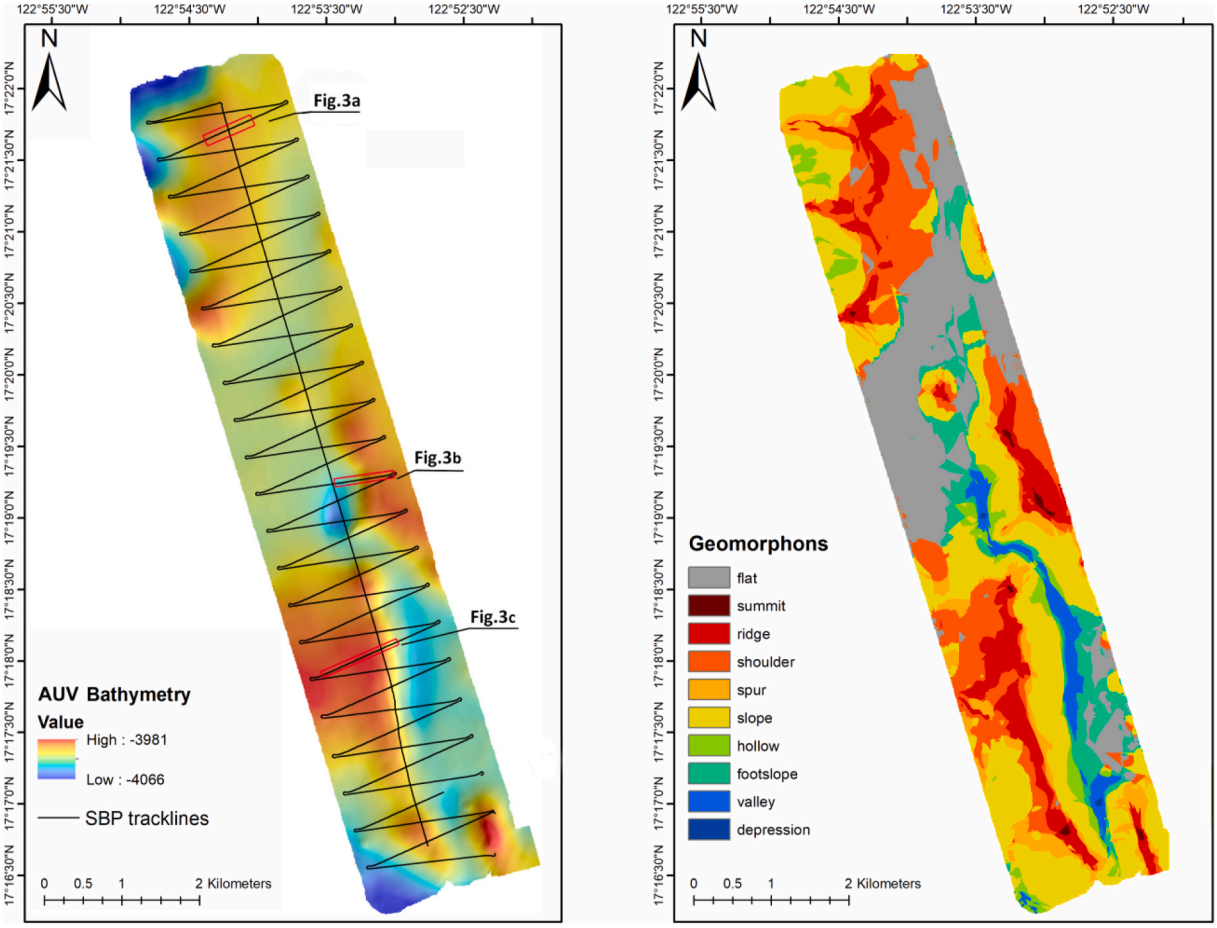

Fig. 2. a) AUV-based MBES bathymetry of the study area and SBP/photography survey track lines, b) Morpho-bathymetric map of the study area resulting from the 'geomorphon' algorithm.

2.2. Fine-scale geomorphology

AUV bathymetry data was used for automatic classification by applying the geomorphons algorithm (Jasiewicz and Stepinski, 2012) as implemented in SAGA GIS. This pattern recognition algorithm classifies a bathymetric digital elevation model (DEM) by examining an adaptive neighbourhood of pixels defined by the following parameters: a) the flatness threshold (equal to 3° here) and b) the line-of-sight range (set to 1000 m). The geometry of each neighbourhood is then matched to a set of reference geomorphometric features for classification. Up to ten major geomorphometric classes may be identified (Fig. 2b). This approach produces fast and reliable results in an objective way, purely based on the data characteristics. Consequently, the geomorphons classes are examined together with sediment thickness for identifying potential geomorphological bias in nodule occurences (see section 4.1).

2.3. Sub-bottom profiles and stratigraphy

The geophysical data used for deriving sediment thickness were collected using an EdgeTech© CHIRP (2–13 kHz) sub-bottom profiler (SBP) mounted on the AUV Autosub6000. The data coverage is shown in Fig. 2a. Sub-bottom profiles cover a dense network of track lines and were collected simultaneously with seafloor photographs from which nodule metrics were extracted (see following paragraph), thus allowing a better interpretation of both datasets. The CHIRP system was recording data using a 5 ms sweep at an altitude of 3 m above the seafloor. The maximum penetration of the signal reaches 15–20 m below the seafloor surface capturing various acoustic reflectors that form the local stratigraphy of the area (Fig. 3). The sub-bottom data were analysed with the Sonarwiz© software and three major acoustic units were identified. The thickness of the top unit (see section 3.2, AU3 unit) was then exported for GIS analyses in tandem with the nodule information extracted from AUV-photographs.

2.4. Seafloor photograph acquisition and analysis

The Autosub6000 was carrying two Grasshopper© cameras (GS2-GE-50S5C model) mounted ca. 70 cm apart facing forward and downward and thus providing an oblique and perpendicular view of the seafloor. Image collection was performed with an AUV speed of 1.2 ms^{-1} and an interval sampling rate of 850 ms. The AUV collected more than 30,000 (useable and non overlapping) downward-looking images in the ridge study area which were further used for identification and measuring of Mn-nodules. The nodule identification from seafloor imagery was conducted by an automatic image analysis algorithm developed by Schoening et al. (2016). Details of the image acquisition and post-processing (e.g. seafloor overlap and dark frame removal) are reported in Simon-Lledóet al. (2019). Accordingly, each seafloor image was geometrically corrected, and scored with image area, number of nodules identified, nodule coverage and nodule size parameters. In this study, we use the nodule density (i.e. nodules m^{-2}), the number of nodules divided by the image area, as a standardized measure for nodule density across the study area. The nodules m^{-2} unit was selected as a robust and objective measure that is not influenced by image-to-image differences in capture geometry. This choice was further favored, since nodule sizes in the study area do not show major variability that could alter the validity of nodule density. Nodule density was supported by countings derived from three box-core samples collected at the study area (Fig. 1b)

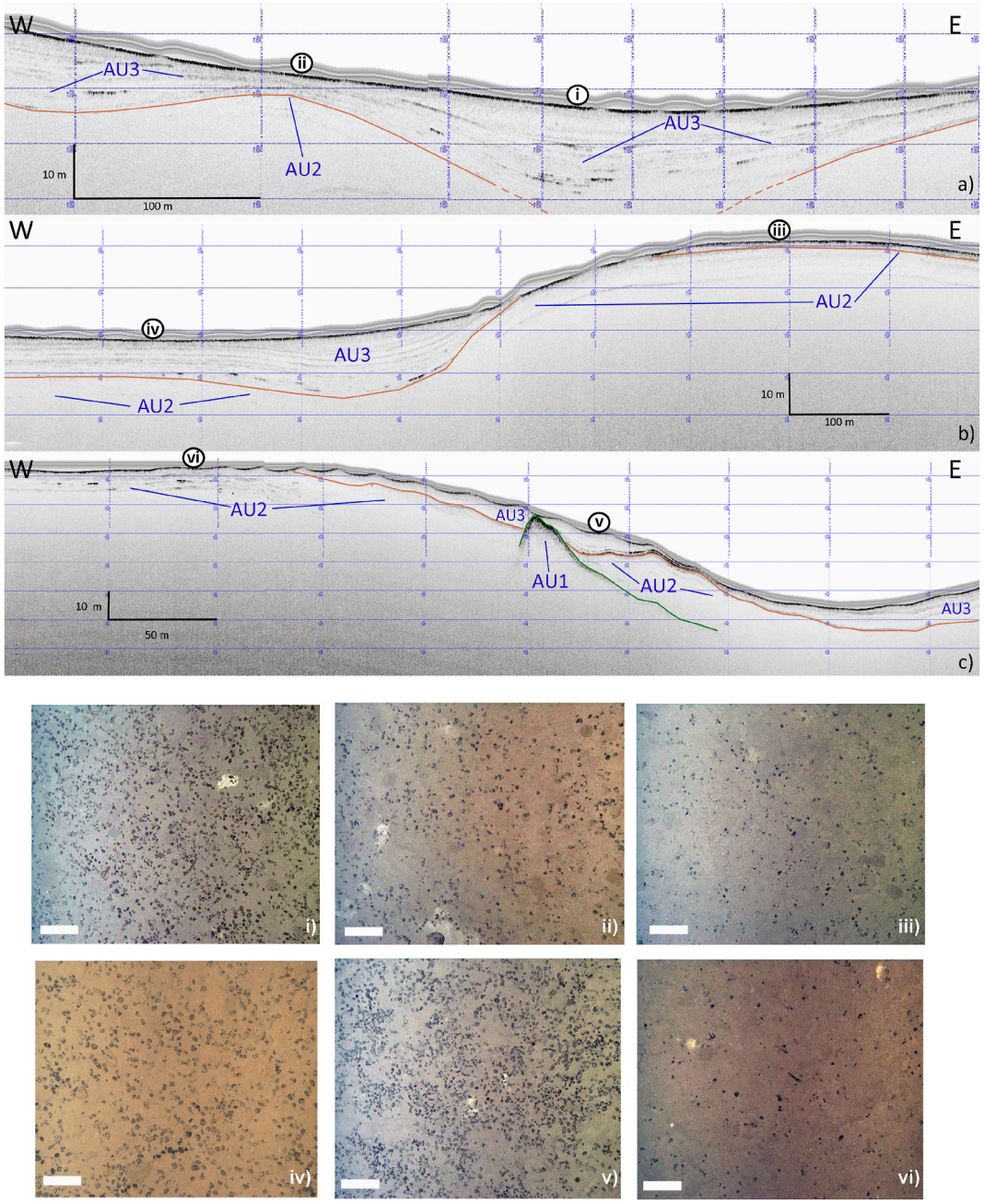

Fig. 3. a,b,c: Selected sub-bottom profiles from the study area (positions shown in Fig. 2a and 4a with red rectangles). Interpretation of acoustic units: AU3: unconsolidated sediments, AU2: consolidated sediments, AU1: bedrock. i-vi: Sample AUV-photographs from selected parts of the SBP data with contrasting AU3 thickness. The white bar refers to a scale of 25 cm.

that are neighboring with AUV-photography. Although, three ground-truth samples are not statistically ideal for validating remotely-sensed imagery, these were the only ones available from within the study area. In order to enhance the analysis of nodule data against the geophysical data (i.e., sediment thickness) the respective nodule metrics were subdivided in three major groups of increasing density according to the values suggested by the natural breaks (jenks) method for estimating class range in ArcMap©. The natural breaks is an optimization method that groups the data into classes with maximum distance between their means (arcgis.com, accessed September 30, 2020). In order to obtain a better overview of the spatial distribution of nodule densities and the sediment thickness, we created interpolated surfaces using the ordinary kriging algorithm (using a logarithmic semivariogram model) from the geostatistical analyst toolbox in ArcMap© 10.6. A more quantitative analysis of the correlation between sediment thickness and nodule density classes was performed by applying a Kruskal-Wallis test.

3. Results

3.1. Geomorphological features

The pattern recognition algorithm revealed various morpho-bathymetric features in the study area (Fig. 2b). In general, the area can be subdivided into northern and southern parts with the northern part containing mainly positive elevation features such as ridges and shoulders surrounded by flat (<3°) plains. The southern part comprises of both positive and negative (valleys and footslopes) features

interleaved with broader slope areas. Particularly, in the southern part, the ridges surround the central valley feature. The spatial pattern of these features can be viewed as an analogue to Horst and Graben structures on a landscape scale.

3.2. Interpretation of sub-bottom profiles

The acoustic stratigraphy of the area comprises of three major acoustic units, tentatively interpreted as bedrock, consolidated sedimentary layers and unconsolidated sediments. Since there is not any gravity-core data with sufficient penetration in the study area, the suggested interpretation is based on earlier literature and in-situ observations from box-core samples collected during the JC120 cruise (Jones et al., 2015). Acoustic Unit 1 (AU1) is represented by the deepest high-amplitude reflectors (Fig. 3c). They occur sparsely and at a few instances they outcrop on or near the seafloor surface. AU1 is probably related to basaltic basement rock (ISA, 2010) and its geometry indicates that it may be linked with escarpments of active faults in the area. A semi-transparent acoustic unit (AU2) with parallel internal geometry possibly represents consolidated sediments of Miocene age (ISA, 2010) that cover large parts of the area. This is further corroborated by evidence presented in Halbach et al. (1988) and Kazmin (2003). Additional evidence is provided by Baláž (2021) and Kotliński and Tkatchenko (1997) regarding a stratified, semi-transparent acoustic layer in the CCZ with a late Miocene to early Miocene age. AU2 is usually covered by the third acoustic unit AU3 in varying thickness (Fig. 3b). AU2 has a gentle slope and can reach the seafloor surface where it is then only covered by a thin veneer of AU3. The exact thickness of AU2 is unclear, since the acoustic signal attenuates quickly. Acoustic unit AU3 is characterized by transparency and occasionally includes fragmented secondary reflectors

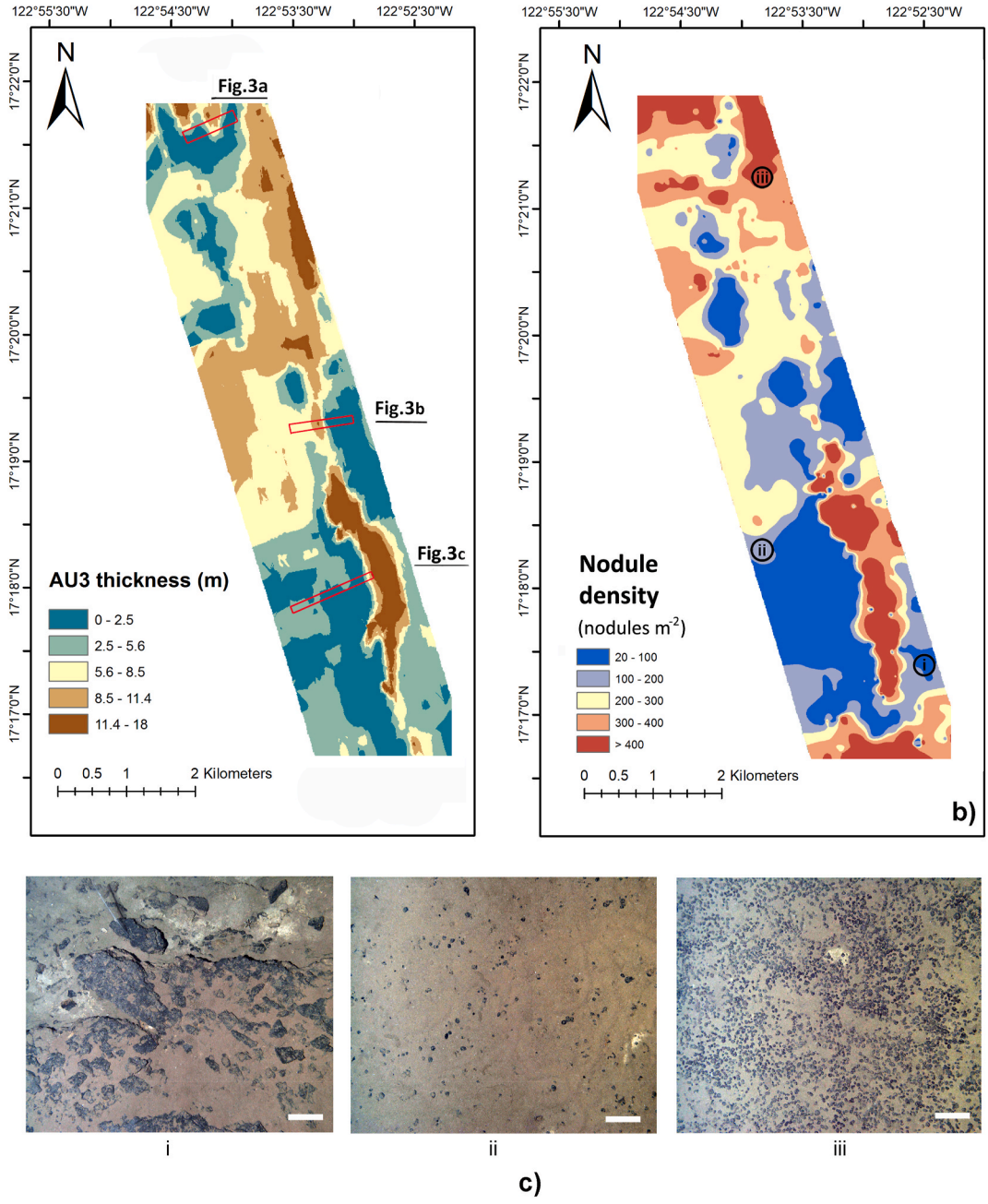

Fig. 4. Ordinary kriging outputs and representative AUV photography: a) Interpolated thickness of digitized AU3, b) interpolated grid of nodule density from AUV imagery data points, c) i) outcropping bedrock AU1, ii) veneer of AU3 with sparse nodules, iii) thick AU3 with dense nodules. The white bar refers to a scale of 25 cm.

(Fig. 3a). This unit has variable thickness, covers large parts of the area and has a maximum thickness of 18 m. It is tentatively interpreted as unconsolidated sediments and it is attributed to siliceous/pelagic clay sediments (Halbach et al., 1988; ISA, 2010; Jones et al., 2015; Jones et al., 2021). Characterization of AU3 was further supported by visual examination of box-core samples during the JC120 cruise (Jones et al., 2015). This is further supported, by earlier geo-acoustic studies at the CCZ area, suggesting the existence of an upper transparent layer with Quaternary age, constituting mainly of siliceous oozes (Kotliński et al., 2009; Baláž, 2021).

3.3. Sediment thickness and characteristics of Mn nodules

Nodule countings from three box-core samples confirm the nodule density estimated from AUV imagery. Although partial burial of nodules has an effect on the apparent nodule density (Tsune, 2021) it is assumed that the low sedimentation rates at the study area should have a minimal burial effect on the nodules. The interpolated maps of AU3 thickness and nodule density show similar patterns (Fig. 4), and the Kruskal-Wallis test showed that the groups of nodule densities correspond with statistically significant, distinctive thicknesses of unit AU3 ($H = 2216$, $df = 2$, $p < 0.001$, $\alpha = 99$, Fig. 5). Essentially, large densities (>250 nodules m^{-2}) of Mn nodules seem to correspond with increased thickness (>6 m) of AU3, covering mainly the '*flat*' and '*valley*' geomorphic units of the study area (Figs. 2b and 4b). Locations where this unit is relatively thin (<6 m thickness) or is absent show lower densities of Mn nodules. The lowest densities of Mn nodules seem to be related with areas where AU1 and AU2 layers reach the seafloor. Based on qualitative evaluation (Fig. 4) and statistical analysis between the nodule densities and the thickness of AU3 it may be inferred that:

A) The lowest nodule densities correspond with thin sediment deposits and/or outcropping substrata whereas the highest nodule densities are found over thicker sediment deposits (Fig. 3; Fig. 5).
B) Locations with increased sediment thickness occur more frequently at the '*flat*' and '*valley*' geomorphological units. On the other hand, areas of low or minimal sediment thickness correspond mostly with the '*ridge*' geomorphological unit.

4. Discussion

4.1. Indicators of past geochemical patterns

Geophysical and image-based analyses suggest that Mn nodule occurrence in this study area is proportional to unconsolidated sediment thickness (Fig. 3; Fig. 5). Where there is no sediment accumulation, notably in areas with positive relief (ridges, shoulders, as classified by the geomorphon algorithm), nodule occurrence is considerably decreased. In contrast, sedimentary layers with moderate thickness occur in both flat and valley areas suggesting that increased nodule densities do not associate with a particular geomorphic feature. These findings are in partial contrast to findings of earlier studies (Glasby et al., 1982; Usui and Tanahashi 1986; Usui et al., 1993), with our results suggesting that locally varying sedimentary patterns may have a strong positive influence on nodule occurrence.

The presence of higher nodule densities (nodules per square meter) on top of thick sedimentary layers (represented by AU3) provides new evidence on the controls of Mn nodule distribution. Although a clear

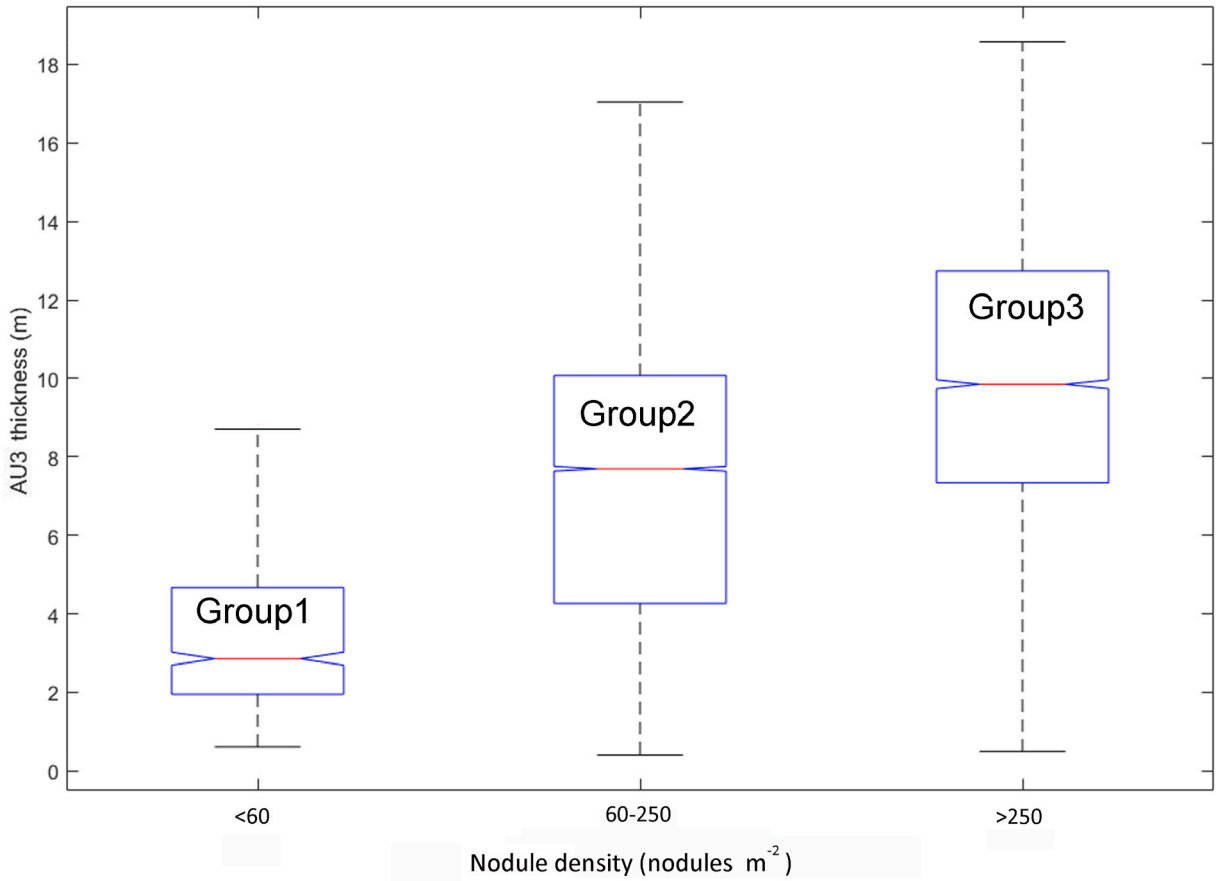

Fig. 5. Box-plot of AU3 (unconsolidated sediment) thickness with nodule density classes (Group1: 715 samples, Group2: 24 400 samples, Group3: 6200 samples, The bottom and top of the blue rectangles represent the 25th and 75th percentiles respectively, whereas the red line indicates the median value. The whiskers extend to the minimum and maximum value of the D50 values that are not considered outliers (i.e., they are no more than ±2.7σ apart).

interpretation of the findings from this study cannot take place without considering any detailed sedimentological or geochemical evidence, we attempt to provide some potential explanations according to literature outcomes based on neighboring areas. The following hypotheses are based on the assumption that thick sedimentary deposits (mainly represented by siliceous clays) at the study area provided an important source for Mn in contrast to consolidated outcrops or thin sedimentary layers. This suggestion is derived from the conceptual model suggested by Hein and Petersen (2013) according to which, deep-seated basaltic rock provides the necessary Mn ions to the geochemically active layer (surface sediments) resulting in growth of mixed types of nodules (hydro- and diagenetic) on sediments with intermediate thickness. One possible scenario that may explain the relation of nodule density with sediment thickness is related to the extent of the oxic zone interface. It has been suggested that when the oxic zone is narrow (e.g.: a few centimetres wide) then sub-oxic, diagenetic nodule growth occurs from upward mobilization of Mn found within thick sedimentary deposits (Mewes et al., 2014; Wegorzewski and Kuhn, 2014; Kuhn et al., 2017; Volz et al., 2020). Considering that the oxic zone at the CCZ was significantly compressed several thousands of years ago (Volz et al., 2020), it is implied that thick and rich in Mn sedimentary layers could have favored the formation of diagenetic nodules. However, this scenario is contradicted by nodule evidence from the study area that suggest a rather hydrogenetic origin of the nodules (Menendez et al., 2019). Particularly, the mineral composition of nodules from our study area suggests a primarily hydrogenetic formation, although the metal ratios in some samples of APEI-6 nodules suggest mixed hydrogenetic and diagenetic growth (Menendez et al., 2019). Thus, suboxic diagenetic nodule growth may only have occurred in a period when the oxic layer was significantly condensed and the pore waters were rich in Mn and other metals. Nevertheless, Menendez et al. (2019) relied on nodule data from samples with large geographic dispersion and thus, their results may not be sufficient to capture fine-scale variability of nodule geochemical properties. An alternative scenario could be that nodule formation may have been fluctuating between hydrogenetic and diagenetic growth. Wegorzewski and Kuhn (2014) proposed that large-scale changes in organic matter flux in the CCZ could have caused alternating oxic/suboxic conditions on the surface sediments which have caused the occurrence of mixed type nodules. Their explanation is based on geochemical analyses of individual nodules which were found to consist of layers with alternating origin. It has to be noted that when sediments are rich in Mn ions, under certain conditions, nodules may precipitate via oxic-diagenetic processes even when the oxic layer is well-developed (Volz et al., 2020). These two scenarios require detailed, fine-scale geochemical analyses both on the nodules and surrounding sediments in order to be validated. A key feature that would assist in discerning hydrogenetic from diagenetic nodules is their size. Nodule sizes (diameters) less than 5 cm are generally considered small (smooth shape) and usually they are of hydrogenetic origin while greater nodule sizes (rough shape) characterize nodules of diagenetic origin (Halbach et al., 1988; Volz et al., 2020). Earlier studies have demonstrated that sediment thickness is an important factor related to nodule abundance and that various nodule types (rough or smooth) are found preferentially on particular sedimentary facies (Usui and Tanahashi, 1992; Tanahashi, 1992). Specifically, Usui & Tanahashi (1992) found that type-r (rough) nodules were mostly correlated with moderate thickness of a particular type of sedimentary layers while type-s (smooth) nodules were mostly found over thin deposits or rocky outcrops. Although large nodules (>4 cm) have been identified by the image analysis algorithm, it was not possible to establish a clear connection between large nodules and a particular sedimentary layer. Furthermore, extracting the size of nodules from underwater photography is not always reliable because partial burial of nodules causes the algorithm to underestimate the exact 2D size of nodules by detecting only the exposed surface of the nodule. Additionally, large rock fragments may induce further bias in the estimation of nodule size from AUV imagery.

It has to be mentioned that sediment thickness is not the only factor affecting the geochemical properties of sediments. Factors such as the organic matter input, availability of electron acceptors and oxygen diffusion from the basaltic basement are having a crucial role in the geochemical processes of the sediments that promote nodule growth (Kuhn et al., 2017). Thus, sediment thickness may be considered as a synergistic parameter, which under certain conditions influences the processes that lead to nodule development.

4.2. Implications for mineral prospecting

Several studies have shown that various geophysical parameters (e.g. bathymetry, backscatter) can be utilized for inferring quantitative information about nodule fields that is useful to the deep-sea mining industry. Peukert et al. (2018) estimated nodule abundance from AUV side-scan sonar imagery and bathymetry classification, and similarly Gazis et al. (2018) combined high-resolution AUV hydro-acoustic datasets for inferring nodule densities over large areas in the Pacific. In particular, both studies found that some bathymetric derivatives (Bathymetric Position Index and slope) were correlated significantly with nodule densities. The apparent correlation between sediment thickness and nodule occurrence in this study suggests that once a causal relationship is validated between the two, then sediment thickness can be used as surrogate variable in estimating indirectly certain mineral quantities such as tonnage and nodule abundance. The potential relationship between thick sedimentary deposits and diagenetic nodules is going to offer valuable input on estimation of tonnage since different nodule types hold specific amounts of minerals (Kuhn et al., 2017). It is implied that in areas where hydrogenetic nodules dominate, it is possible to observe different correlations between nodule abundance and fine-scale bathymetric features. This is explained by the fact that near-bottom hydrodynamics should interact with bathymetry (and vice-versa) in a way that favours hydrogenetic nodule growth. Consequently, it is hypothesized that in areas where diagenetic nodules dominate, a correlation of nodule abundance with sedimentary features and primarily sediment thickness is expected. This is probably because sedimentary layers act as Mn source which under suitable geochemical conditions supports nodule development.

The findings from this study contribute further to the knowledge accumulated by previous work within the MIDAS project. Particulary, this work provides a new aspect in Mn nodule studies by highlighting the role of local sediment thickness variations in promoting nodule growth. This is particularly important since the MIDAS project focuses on promoting interdisciplinary research for advancing the understanding of processes in deep sea Mn nodule fields. The observed evidence resulted by exploiting state-of-the-art geophysical imaging of the seafloor (thus capitalizing on the technology supported by the MIDAS project) and provides new hypotheses to be explored by future deep sea studies.

4.3. Implications on deep sea benthic habitats

Deep-sea nodule fields are an unusual mosaic habitat where the combination of the hard substratum provided by nodules and the background sediment increases habitat complexity (Simon-Lledó et al., 2019), promoting the development of unique and highly diverse benthic communities (Glover et al., 2002; Amon et al., 2016; Gooday et al., 2017; Simon-Lledó et al., 2020). Variations in seabed geomorphology and in nodule availability drive significant variations in megafaunal density and community composition in APEI-6 (Simon-Lledó et al., 2019), as appears to be commonplace at the CCZ (Simon-Lledó et al., 2020). Previous studies from APEI-6 have shown that local distributions of particular animal groups, such as suspension feeding fauna (e.g. anemones or soft corals) were highly influenced by variations in nodule availability (Simon-Lledó et al., 2019). The results of this study suggest that variations in sediment thickness may be inherently influencing key ecological features by controlling nodule occurrence. Hence such

stratigraphic data may be considered as a potential proxy for explaining and predicting biological variations in faunal density and composition in future studies.

4.4. Future work

Geophysical data collected with AUV provide a basis for reconsidering the role of sediment thickness and local lithology in nodule development. However, secure inferences and conclusions cannot result from geophysical data alone. In order to further validate the findings from this study, a comprehensive set of geochemical data from several locations of variable sediment thickness should be collected. High-resolution local geochemical data may provide indications about past sedimentation rates and redox conditions and explain better the nodule variability in type and abundance. It is proposed that future studies take into consideration the local patterns of sedimentary layers along with nodule samples and sizes from sediments with contrasting thicknesses. This way, the potential influence of sediment thickness on nodule growth will be better evaluated. The study of Wegorzewski and Kuhn (2014) is a good example which could be applied on samples from a local neighbourhood, and not only on single-point samples. Therefore it is suggested that nodule geochemical sampling should follow a pattern so that nodules from representative sedimentary layers are examined. Ideally, this type of sampling should be facilitated at a number of sites with different geographic settings for validating the results at a regional scale.

5. Conclusions

Current deep-sea mapping technology has changed the way of imaging the spatial distribution of Mn nodules and accordingly, new concepts arise regarding nodule growth and occurrence. The data from this study allowed mapping of subsurface units and demonstrated that nodule density variations are related to local variations of sediment thickness. The main outcome of this study is that the role of sediment thickness in nodule occurrence is probably more influential than previously thought, and that geochemical (nodules and sediments) and sedimentological data of high spatial resolution are required for assessing this relationship. Thus, future work should focus on the coupling between sediment thickness and nodule type from a geochemical perspective, by applying a more detailed sampling of the sedimentary layers and nodules, in both horizontal and vertical scales than has been achieved until now.

Declaration of competing interest

The authors declare that they have no known competing financial interests or personal relationships that could have appeared to influence the work reported in this paper.

Acknowledgments

This work was based on data collected for the project: Managing Impacts of Deep-seA reSource exploitation (MIDAS), grant agreement 603418 which was supported by the European Union Seventh Framework Programme (FP7/2007–2013). Additional support was provided by the UK Natural Environment Research Council as part of the National Capability Programme and the Marine Environmental Mapping Programme (MAREMAP). We thank the ships' company of RRS James Cook and personnel involved from OBE, MG and NMF at NOC for their help and support. In addition we would like to thank Anna Lichtschlag and Rachael H. James for their valuable discussions and feedback on this manuscript. Datasets used in this study are provided as supplementary material for review purposes. These datasets will become available on an online repository in the following website https://www.bodc.ac.uk/.

References

Amon, D.J., Ziegler, A.F., Dahlgren, T., Glover, A., Goineau, A., Gooday, A.J., Wiklund, H., Smith, C.R., 2016. Insights into the abundance and diversity of abyssal megafauna in a polymetallic-nodule region in the eastern Clarion-Clipperton Zone. Nat. Sci. Rep. 6, 30492. https://doi.org/10.1038/srep30492.

Baláž, P., 2021. Results of the First Phase of the Deep-Sea Polymetallic Nodules Geological Survey in the Interoceanmetal Joint Organization Licence Area (2001–2016). Mineralia Slovaca, pp. 3–36. Web ISSN 1338-3523, ISSN 0369-208653.

Chakraborty, B., Pathak, D., Sudhakar, M., Raju, Y.S., 1996. Determination of nodule coverage parameters using multibeam normal incidence echo characteristics: a study in the Indian ocean. Mar. Georesour. Geotechnol. 15, 33–48. https://doi.org/10.1080/10641199709379933.

de Moustier, C., 1985. Inference of manganese nodule coverage from Seabeam acoustic backscattering data. Geophysics 50, 989–1005.

Frazer, J.Z., Fisk, M.B., 1981. Geological factors related to characteristics of sea-floor manganese nodule deposits, Deep Sea Research Part A. Oceanographic Research Papers 28 (12), 1533–1551. https://doi.org/10.1016/0198-0149(81)90096-0.

Gazis, I.-Z., Schoening, T., Alevizos, E., Greinert, J., 2018. Quantitative mapping and predictive modeling of Mn nodules' distribution from hydroacoustic and optical AUV data linked by random forests machine learning. Biogeosciences 15, 7347–7377. https://doi.org/10.5194/bg-15-7347-2018.

Glasby, G.P., Stoffers, P., Sioulas, A., 1982. Manganese nodule formation in the Pacific Ocean: a general theory. Geo Mar. Lett. 2, 47. https://doi.org/10.1007/BF02462799.

Glover, A.G., Smith, C.R., Paterson, G.L.J., Wilson, G.D.F., Hawkins, L., Sheader, M., 2002. Polychaete species diversity in the central Pacific abyss: local and regional patterns, and relationships with productivity. Mar. Ecol. Prog. Ser. 240, 157–170.

Gooday, A.J., Holzmann, M., Caulle, C., Goineau, A., Kamenskaya, O., Weber, A.A.T., Pawlowski, J., 2017. Giant protists (xenophyophores, Foraminifera) are exceptionally diverse in parts of the abyssal eastern Pacific licensed for polymetallic nodule exploration. Biol. Conserv. 207, 106–116.

Halbach, P., Friedrich, G., Stackelberg, U.V., 1988. The Manganese Nodule Belt of the Pacific Ocean: Geology, Environment, Nodule Formation, and Mining Aspects. Ferdinand Enke Verlag, Stuttgart, Germany, p. 1-254.

Hein, J.R., Petersen, S., SPC, 2013. Deep Sea Minerals: manganese Nodules, a physical, biological, environmental, and technical review. In: Baker, E., Beaudoin, Y. (Eds.), Secretariat of the Pacific Community \, 1B.

ISA, 2010. A Geological Model of Polymetallic Nodule Deposits in the Clarion-Clipperton Fracture Zone, 2010. Technical Study: No. 6. eBook by the International Seabed Authority, Kingston. ISBN: 978-976-95268-2-2.

Jasiewicz, J., Stepinski, T.F., 2012. Geomorphons — a pattern recognition approach to classification and mapping of landforms. Geomorphology 182, 147–156. https://doi.org/10.1016/j.geomorph.2012.11.005, 2013.

Jones, D.O.B., et al., 2015. RRS James Cook Cruise JC120 15 Apr–19 May (2015), Manzanillo to Manzanillo, Mexico. Managing Impacts of Deep-Sea Resource Exploitation (MIDAS): Clarion-Clipperton Zone North Eastern Area of Particular Environmental Interest. Report 32, 117. NOC, Southampton, UK.

Jones, D.O.B., Simon-Lledo, E., Amon, D.J., Bett, B.J., Caulle, C., Clément, L., Connelly, D.P., Dahlgren, T.G., Durden, J.M., Drazen, J.C., Felden, J., Gates, A.R., Georgieva, M.N., Glover, A.G., Gooday, A.J., Hollingsworth, A.L., Horton, T., James, R.H., Jeffreys, R.M., Laguionie-Marchais, C., Leitner, A.B., Lichtschlag, A., Marsh, L., Menendez, A., Paterson, G.L.J., Peel, K., Robert, K., Schoening, T., Shulga, N., Smith, C.R., Taboada, S., Thurnherr, A.M., Wiklund, H., Young, C.R., Huvenne, V.A.I., 2021. Environment, ecology, and potential effectiveness of an area protected from deep-sea mining (Clarion Clipperton Zone, abyssal Pacific). Prog. Oceanogr.

Kazmin, Y.B., 2003. Geology of the clarion-clipperton fracture zone (CCZ) – existing geologic information in respect of polymetallic nodules in the CCZ. In: Meeting of Workshop to Develop a Geological Model of the Clarion-Clipperton Polymetallic Nodule Deposits, Fiji Islands. held by International Seabed Authority. May 13 - 20.

Kotliński, R.A., Tkatchenko, G., 1997. Preliminary results of IOM environmental research. In: Proc. Int. Symposium on Environmental Studies for Deep-Sea Mining. Metal Mining Agency Japan, Tokyo, pp. 35–44.

Kotliński, R.A., Yubko, V., Stoyanova, V., 2009. Effects of the Structural-Tectonic and Volcanic Processes on Formation of Polymetallic Nodules in the CCZ. Presentation from the Workshop on the Finalization of the Geological Model of the Clarion-Clipperton Fracture Zone (CCZ). Authority's Headquarters in Kingston, Jamaica.

Kuhn, T., Wegorzewski, A., Rühlemann, C., Vink, A., 2017. In: InDeep-SeaMining, Sharma, R. (Eds.), Composition, Formation, and Occurrence of Polymetallic Nodules. Springer International Publishing, Basel, Switzerland, pp. 23–63.

Kwasnitschka, T., Köser, K., Sticklus, J., Rothenbeck, M., Weiß, T., Wenzlaff, E., Schoening, T., Triebe, L., Steinführer, A., Devey, C., Greinert, J., 2016. DeepSurveyCam—a deep ocean optical mapping system. Sensors 16, 164.

Le Gal, L., Edy, C., 1997. CARAIBES: an integrated software for multibeam echosounder and sides can sonar data mapping. In: Oceans '97. MTS/IEEE Conference Proceedings, 2, pp. 1242–1245. https://doi.org/10.1109/OCEANS.1997.624173.

Lee, S.H., Kim, K.H., 2004. Side-scan sonar characteristics and manganese nodule abundance in the Clarion-Clipperton Fracture Zones NE equatorial Pacific. Mar. Georesour. Geotech 22, 103–114.

Martin-Barajas, A., Lallier-Verges, E., Leclaire, L., 1991. Characteristics of manganese nodules from the Central Indian Basin: relationship with the sedimentary environment. Mar. Geol. 101 (1–4), 249–265. https://doi.org/10.1016/0025-3227(91)90074-E.

Menendez, A., James, R.H., Lichtschlag, A., Connelly, D., Peel, K., 2019. Controls on the chemical composition of ferromanganese nodules in the Clarion-Clipperton Fracture Zone, eastern equatorial Pacific. Mar. Geol. 409 (1), 14. https://doi.org/10.1016/j.margeo.2018.12.004. ISSN 0025-3227.

Mewes, K., Mogollón, J.M., Picard, A., Rühlemann, C., Kuhn, T., Nöthen, K., Kasten, S., 2014. Impact of depositional and biogeochemical processes on small scale variations in nodule abundance in the Clarion-Clipperton Fracture Zone. Deep Sea Res. Part I 91 (125–141), 125–141. https://doi.org/10.1016/j.dsr.2014.06.001. ISSN 0967-0637.

Moore, T.C., Heath, G.R., 1966. Manganese nodules, topography, and thickness of Quaternary sediments in the Central Pacific. Nature 212, 983–985.

Morris, K.J., Bett, B.J., Durden, J.M., Huvenne, V.A.I., Milligan, R., Jones, D.O.B., McPhail, S., Robert, K., Bailey, D.M., Ruhl, H.A., 2014. A new method for ecological surveying of the abyss using autonomous underwater vehicle photography. Limnol Oceanogr. Methods 12, 795–809.

Okazaki, M., Tsune, A., 2013. Exploration of polymetallic nodule using AUV in the central equatorial pacific. Proceedings of the Tenth ISOPE Ocean Mining and Gas Hydrates Symposium, Szczecin, Poland 2013, 22–26 September.

Pennington, J.T., Mahoney, K.L., Kuwahara, V.S., Kolber, D.D., Calienes, R., Chavez, F.P., 2006. Primary production in the eastern tropical Pacific: a review. Prog. Oceanogr. 69, 285–317.

Peukert, A., Schoening, T., Alevizos, E., Köser, K., Kwasnitschka, T., Greinert, J., 2018. Understanding Mn-nodule distribution and evaluation of related deep-sea mining impacts using AUV-based hydroacoustic and optical data. Biogeosciences 15, 2525–2549. https://doi.org/10.5194/bg-15-2525-2018.

Piper, D.Z., Blueford, J.R., 1982. Distribution, mineralogy, and texture of manganese nodules and their relation to sedimentation at DOMES Site A in the equatorial North Pacific. Deep-Sea Res. 29, 927–952.

Schoening, T., Kuhn, T., Jones, D.O.B., Simon-Lledo, E., Nattkemper, T.W., 2016. Fully automated image segmentation for benthic resource assessment of poly-metallic nodules. Methods Oceanogr 15/16, 78–89. https://doi.org/10.1016/j.mio.2016.04.002.

Shirayama, Y., Itoh, H., Fukushima, T., 2017. Recent developments in environmental impact assessment with regard to mining of deep-sea mineral resources. In: Sharma, R. (Ed.), Deep-Sea Mining. Springer, Cham. https://doi.org/10.1007/978-3-319-52557-0_15.

Simon-Lledó, E., Bett, B.J., Huvenne, V.A.I., Schoening, T., Benoist, N.M.A., Jones, D.O.B., 2019. Ecology of a polymetallic nodule occurrence gradient: implications for deep-sea mining. Limnol. Oceanogr. 64, 1883–1894.

Simon-Lledó, E., Pomee, C., Ahokava, A., Drazen, J.C., Leitner, A.B., Flynn, A., Parianos, J., Jones, D.O.B., 2020. Multi-scale variations in invertebrate and fish megafauna in the mid-eastern Clarion Clipperton Zone. Prog. Oceanogr. 187, 102405. https://doi.org/10.1016/j.pocean.2020.102405. ISSN 0079 6611.

Smith, C.R., Demopoulos, A.W.J., 2003. The deep Pacific Ocean floor. In: Tyler, P.A. (Ed.), Ecosystems of the Deep Oceans: Vol 28 (Ecosystems of the World). Elsevier Science Ltd, London.

Tanahashi, M., 1992. Subsurface Acoustic Layers Detected by 3.5 kHz Subbottom Profiler in the Southern Part of the Central Pacific Basin (GH82-4 Area, 22. Geological Survey of Japan Cruise Report, pp. 29–38.

Tsune, A., 2021. Quantitative expression of the burial phenomenon of deep seafloor manganese nodules. Minerals 11, 227. https://doi.org/10.3390/min11020227.

Usui, A., Tanahashi, M., 1986. The relationship of local variation of manganese nodule deposits to acoustic stratigraphy in the GH82–4 area, southern Central Pacific Basin. Geological Survey of Japan Cruise Report 21, 160–161 70.

Usui, A., Tanahashi, M., 1992. The Relationship of Local Variation of Manganese Nodule Deposits to Acoustic Stratigraphy in the GH82–4 Area, Southern Central Pacific Basin, 22. Geological Survey of Japan Cruise Report, pp. 219–231.

Usui, A., Nishimura, A., Iizasa, K., 1993. Submersible observations of manganese nodule and crust deposits on the Tenpo Seamount, Northwestern Pacific. Mar. Georesour. Geotechnol. 11 (4), 263–291. https://doi.org/10.1080/10641199309379924.

Volz, J.B., Liu, B., Köster, M., Henkel, S., Koschinsky, A., Kasten, S., 2020. Post-depositional manganese mobilization during the last glacial period in sediments of the eastern Clarion-Clipperton Zone, Pacific Ocean. Earth Planet Sci. Lett. 532 (116012) https://doi.org/10.1016/j.epsl.2019.116012.

Wegorzewski, A.V., Kuhn, T., 2014. The influence of suboxic diagenesis on the formation of manganese nodules in the Clarion Clipperton nodule belt of the Pacific Ocean. Mar. Geol. 357, 123–138. https://doi.org/10.1016/j.margeo.2014.07.004. ISSN 0025-3227.

Weydert, M., 1990. Measurements of the acoustic backscatter of selected areas of the deep seafloor and some implications for the assessment of manganese nodule resources. J. Acoust. Soc. Am. 88, 350–366.

Wynn, R.B., Huvenne, V.A.I., Le Bas, T.P., Murton, B.J., Connelly, D.P., Bett, B.J., Ruhl, H.A., Morris, K.J., Peakall, J., Parsons, D.R., Sumner, E.J., Darby, S.E., Dorrell, R.M., Hunt, J.E., 2014. Autonomous Underwater Vehicles (AUVs): their past, present and future contributions to the advancement of marine geoscience. Mar. Geol. 352, 451–468.